International Journal of Industrial Chemistry (2019) 10:145–158
https://doi.org/10.1007/s40090-019-0180-9

RESEARCH

Amine contaminants removal using alginate clay hybrid composites and its effect on foaming

Anjali Achazhiyath Edathil[1] · Priyabrata Pal[1] · Fawzi Banat[1]

Received: 2 July 2018 / Accepted: 14 March 2019 / Published online: 21 March 2019

Abstract

Heat stable salts such as total organic acids (TOA) and heavy metals are well known contaminants in the acid gas removal systems operating using alkanolamines such as methyldiethanolamine (MDEA, 50 wt%). Decontamination of TOA and heavy metals from lean MDEA always remain as a challenge to the gas industry, as accumulation of TOA deteriorates the solvent quality, weakens the absorption capacity and enhances foaming problems leading to huge loss of MDEA and presence of heavy metals results in corrosion and fouling of equipment. Equilibrium batch adsorption were carried out using calcium alginate clay hybrid composites (CAH) containing sepiolite and bentonite for assessing the sorption performance of TOA and heavy metals such as chromium and iron from industrial lean MDEA solutions. The physiochemical properties of the adsorbent were elucidated using SEM, EDX and FTIR analysis. The effects of operational parameters such as amount of sorbent, contact time and temperature on the sorption capacity were also investigated. Kinetics results indicated that the chemisorption nature. The pseudo-second order model gave the best fit. The adsorption efficiency increased with increasing the temperature. Adsorption followed type VI isotherm according to the IUPAC classification, with sorption taking place in different stages. Regeneration studies revealed that 4% $CaCl_2$ acts as an effective eluting agent and no reduction in capacity was observed even after 3 cycles of regeneration. Foaming studies carried out with treated lean MDEA confirmed the reduction in foam of MDEA solutions owing to the effective removal of foam creators such as TOA from lean MDEA by CAH composites. A 15.8% reduction in TOA content was found to decrease the foam height by 37.5%. Thus, CAH composites containing bentonite and sepiolite are having the potential to reclaim industrial lean MDEA solutions.

Keywords Alginate · Clay composites · Adsorption · Lean amine · Foaming

Introduction

Amine systems employing alkanolamines such as methyldiethanolamine (MDEA) for acid gas absorption are fronting continuous challenge for maintaining and increasing the process throughput and profit. However, the presence of contaminants such as heat stable salts (HSS) and heavy metal ions hinders the smooth operation and causes system downtime and upsets [1]. These HSS are formed by the interaction of MDEA with acid gases (H_2S and CO_2), followed with reaction of the formed protonated MDEA ($MDEAH^+$) with strong acid anionic species such as formate, acetate, propionate, thiosulfate etc. and cannot be regenerated by the application of heat [2]. The accumulation of HSS in the amine deteriorates the solvent quality, reduces the H_2S absorption capacity and augments the foaming leading to significant loss of MDEA [3, 4]. On the other hand, metal contaminants produced from the makeup water or due to the corrosion or erosion caused during the continuous running of the plant results in the fouling of the equipment. Therefore, amine reclamation by reducing these impurities to lower levels have become a necessary step that the gas industry needs to be employed for dramatically improving the operation.

Electronic supplementary material The online version of this article (https://doi.org/10.1007/s40090-019-0180-9) contains supplementary material, which is available to authorized users.

✉ Priyabrata Pal
pal.priyabrata@ku.ac.ae

✉ Fawzi Banat
fawzi.banat@ku.ac.ae

[1] Department of Chemical Engineering, Khalifa University, P.O. Box 127788, Abu Dhabi, United Arab Emirates

Few attempts are reported in literature for the removal of HSS degradation product and heavy metal ions from contaminated amine solutions utilizing services of neutralization [5], vacuum distillation [6], electro dialysis [7–9], ion-exchange [10, 11], and adsorption [12–14]. Among these, adsorption using solid sorbents have drawn significant interest owing to their high removal efficiency, ability to remove even traces of contaminants and low operation, installation and regeneration cost.

Recently, researchers have intensified their investigations with quest for identifying relatively low cost and biodegradable materials with high sorption capacities, so called the green sorbents for contaminant removal from industrial lean amine [15, 16]. This growing demand has paved the way for utilizing alginate, a widely available polysaccharide harvested from marine brown algae [17] as the starting material for making environmentally benign adsorbents [18–20]. Alginates have the ability to form hydrogels, which can hold large amount of water on crosslinking with metal ions. These hydrogel are three-dimensional networks consisting of carboxylic (–COOH) and hydroxyl (–OH) groups, which facilitate the simultaneous removal of heavy metals and total organic acids from industrial lean MDEA (LA) solutions through ion exchange and electrostatic interaction respectively. However, both gel and dry form of the alginate has limitations such as low mechanical strength and swelling problems, respectively and thus causing operational difficulties [21].

Researchers have recently conceptualized the idea of combining relatively low cost clay materials with environmentally friendly alginate for yielding a new class of hybrid materials called bio composites, and thus, curtailing the congenital problems accompanying the alginate sorbents. The effective composite material developed by incorporating alginate into the network of layered silicates belonging to the smectite family such as montmorillonites, bentonite and microfibrous clays such as sepiolite was reported to have the highest sorption capability for the simultaneous removal of TOA and heavy metals from industrial lean amine solutions [22]. Recent studies reported by Alhseinat et al. [23], confirmed the significant effect of various organic acids on the foaming behavior. However, no studies are reported pertaining to understanding the effect of adsorptive removal of total organic acid (TOA) from lean MDEA solutions and its impact on lessening the foaming problems faced in gas sweetening units using alkanolamines. Moreover, the removal of heavy metals such as chromium and iron are also important for preventing the corrosion of the sweetening units.

This work aims to evaluate the potentiality of the contaminant (TOA anions and heavy metal ions) removal from industrial lean MDEA solutions by adsorption using alginate clay composites containing bentonite (CAB) and sepiolite (CAS) and understand its effect on amine foaming. To the best of authors' knowledge, there are no reported literature that address MDEA foamability and adsorption together. The adsorption and desorption capacities of CAB and CAS composites were assessed in detail using equilibrium batch adsorption experiments. Efforts were also paved on investigating the influence of operational factors such as adsorbent dosage, time and temperature on the sorption capacity. SEM, FTIR and EDX analysis were utilized to understand the sorption mechanism and underlying principle; whilst the rate controlling steps were elucidated using uptake kinetics. Furthermore, the potentiality of the contaminant remediation on amine foaming was evaluated through foaming studies.

Experimental

Materials

91% food grade sodium alginate with a characteristic viscosity of 45×10^{-3} Pa s for 1% solution in water was purchased from Loba Chemie, India. Calcium chloride dihydrate of reagent grade was obtained from Merck KGaA, Germany and used as received as a curing agent. Clays such as Na-bentonite, montmorillonite (MMT) and sepiolite were supplied by Alfa Aesar and Sigma Aldrich, respectively. Na^+-type of montmorillonite and sepiolite were prepared in the laboratory using the method reported earlier [22]. Industrial lean MDEA samples containing 50 weight% Methyldiethanolamine were collected from local gas processing industries in UAE.

Methods

Preparation of calcium alginate clay hybrid (CAH) composites

The procedure for the preparation of CAH composites were as described earlier [22]. Briefly, the fabrication of the CAH composites was achieved in three steps: (1) First, a homogeneous solution of alginate containing uniformly dispersed Na^+-clay materials was prepared by agitating sodium alginate (1%, w/v) and Na^+-clay (2%, w/v) in deionized water overnight at 500 rpm. (2) This homogeneous solution was dropped into 1.5 M $CaCl_2$ solution resulting in the formation of beads. The beads were then left in $CaCl_2$ bath for overnight to ensure sufficient crosslinking by the diffusion of Ca^{2+} ions. (3) Finally, the beads were washed three times with deionized water to remove any unreacted calcium ions and dried at room temperature for 2 h before storing in an air tight container for further use. The resulting beads were designated as 2%-CAH, where H represents B for bentonite, M for montmorillonite and S for sepiolite clays, respectively.

The schematic drawing of the preparation of alginate clay composites is as shown in Fig. 1. Similarly, each composites were prepared twice and used for adsorption in same batch of lean MDEA to confirm the reproducibility of the process.

Determination of contaminants in lean MDEA

The UV–Vis spectrophotometer (DR5000, Hach Lange) was used to quantify the total organic acid (TOA) anions present in the industrial LA (lean MDEA) solution. The detailed analytical procedure were described in our previous literatures [21, 22]. The concentration of TOA was found to be 3745 ± 0.5 mg/L. Inductively coupled plasma optical emission spectroscopy (ICP-OES, Optima 8000; Perkin Elmer) was used to quantify the major metal ions present in the lean MDEA. Prior to the analysis, an internal standard of 1.0 mg/L yttrium was added to the LA solution for correcting the physical interference of organic (MDEA)-aqueous mixture [12]. Briefly, the internal standard corrects the following: (1) the viscosity variations of the MDEA aqueous solution which can affect the pumping efficiency of the sample (amount being delivered to the nebulizer) and (2) the surface tension variations of the solutions being aspirated which affect the nebulization efficiency of the sample (amount being vaporized into the spray chamber). The received LA solvent was found to have 1517 ± 0.4 µg/L of chromium and 2697 ± 0.35 µg/L of iron.

Batch adsorption experiments

Batch experiments were performed by adding a known weight of three different CAH adsorbents and 10 mL of lA solution into a 25 mL stoppered conical flasks at the desired experimental condition. The flasks were then placed on a water bath shaker (Dihan, Korea) running at 140 rpm and equilibrated for 4 h as obtained from kinetic behavior. The CAH composites were then separated and the LA samples were filtered using 0.1 µm polytetrafluoroethylene (PTFE) filters prior to the TOA and heavy metal analysis. The equilibrium concentration of TOA and heavy metals were determined using Test kit LCK 365 in UV–VIS and ICP-OES, respectively. The removal efficiency and the uptake capacity of contaminants adsorbed per unit mass on the hybrid composite at equilibrium, q_e (mg/g or µg/g) was determined using following equation:

$$\text{Removal efficiency}\,(\%) = \left(\frac{C_0 - C_e}{C_0}\right) \times 100 \tag{1}$$

$$q_e = \frac{V}{m}(C_0 - C_e) \tag{2}$$

where C_0 and C_e are the initial and equilibrium concentration (mg/L) of TOA/metal ions in LA solution, respectively, (V) is the volume of LA solution (L) and (m) is the mass of different CAH adsorbent. The effect of adsorbent dosage, contact time and temperature on the sorption capacity was assessed using the aforementioned batch adsorption method.

For kinetic studies, 2.0 g of CAH composites were added to 10 mL of lean MDEA taken in different 25 mL conical flasks and were allowed to agitate on a water bath at 140 rpm and 25 °C. Each of the flasks were withdrawn at predetermined time intervals and filtered lean MDEA samples were immediately analyzed for quantifying the residual concentration of TOA/metal ions. All the experiments were triplicated to get the standard deviation within 2.0%.

Desorption experiments

To understand the efficacy of the adsorbent, desorption experiments were carried out using various concentration of $CaCl_2$ as desorbing agent. 2.0 g of TOA and metal loaded CAH composites were suspended in 10 mL of desorption medium taken in a 25 mL conical flask. The flask was then shaken in a water bath at 160 rpm for 15 min followed by a 10 mL water wash for 10 min. The beads were then dried at room temperature for 15 min and used for further adsorption studies to calculate the efficiency of utilized desorption method using the following equation:

$$\text{Desorption efficiency}\,(\%) = \left(\frac{R_c}{R_{fresh}}\right) \times 100 \tag{3}$$

where R_{fresh} and R_c represents the % removal obtained by fresh and after any adsorption–desorption cycle 'c' which was calculated using Eq. (1).

After identifying the best concentration of $CaCl_2$ as regenerant, three consecutive adsorption–desorption cycles were performed to identify the potentiality of the adsorbent. Also, further desorption studies were performed using the

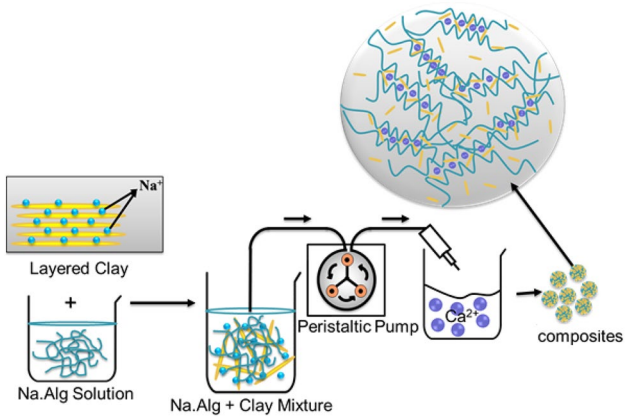

Fig. 1 Schematic of the preparation of alginate clay composites

batch equilibration technique in the following manner: the total mass of 17.0 g CAH composite used in each batch of adsorption experiment, which was used previously for the adsorption study were placed in a 85 mL 4% or used $CaCl_2$ at 25 °C, with a shaking speed of 160 rpm for 15 min. The samples were then washed with deionized water (85 mL) and subjected to three consecutive adsorption–desorption cycles for assessing the reusability of the composites.

Adsorbent characterization

Scanning Electron Microscopy (SEM, FEI Quanta, FEG250, USA) equipped with energy-dispersive x-ray spectroscope (EDX) was used to record the images describing the surface morphology of the Na^+-clay and prepared hybrid composites (before and after adsorption). A few nm sputter gold coating was performed on the surface of the composite prior to the analysis. The Fourier-transform infrared spectroscopy (FTIR) of the pristine and contaminant adsorbed CAH composites were recorded in the range from 4000 to 400 cm^{-1} using Nicolet-6700 ATR-FTIR spectrophotometer with 64 scans and resolution.

Foaming studies

Foaming studies were carried out in an experimental setup that was designed and manufactured based on the pneumatic method. The standard ASTM D892 method that was utilized for performing the foaming tests of lubricating oils (ASTM, 1999) was modified. As illustrated in Fig. 2, the setup consists of a glass column with a height, $H = 19.8$ cm, an inner diameter of $D = 5.4$ cm and consists of six sample ports located at equal distance of 2.5 cm along the foam riser. Prior to each experiment, a gas diffuser was inserted into the glass column. A total of 150 mL of LA samples was pumped into glass column using a peristaltic pump through sample point 6 and left at room temperature for 20 min to reach thermal equilibrium. Compressed dry air at a flux of 22.9 mL/(cm^2 min) was used to disperse gas bubbles to the tested amine solution to obtain the steady foam. All the experiments were repeated thrice to obtain the result.

Results and discussion

The alginate based composites with Na^+-clay (such as bentonite, montmorillonite, and sepiolite) as fillers were successfully synthesized using in situ solution polymerization. The dropping of homogenous sodium alginate-clay mixture into $CaCl_2$ solution results the formation of spherical beads through crosslinking. The adsorption experiments were performed with same batch of lean amine samples using two batches of same type of CAH composites and was found to be a deviation of less than 2.0%. These result further justify the reproducibility of prepared CAH composites.

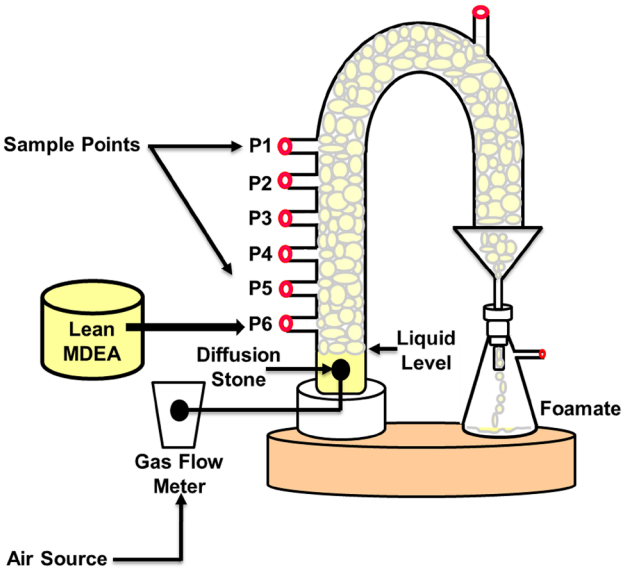

Fig. 2 Schematic diagram for continuous foam fractionation setup

Characterization

SEM analysis of clay and CAH composites

The representative SEM micrographs of fresh, contaminant adsorbed and desorbed composites are shown in Fig. 3. The evaluation of the SEM images of fresh composites confirmed the significant difference on the microstructure owing to the presence of underlying clay particles. A homogeneous distribution of clay particles was attained in the alginate matrix of the composites, irrespective of the clay type. This was achieved by the stabilizing effect showcased by the alginate in the solution state, in turn preventing the agglomeration of clay particles. However, the interruption of sectional alginate chain formation during crosslinking by the uniformly suspended Na^+-clay materials in alginate solution resulted in altering the surface characteristics of alginate hydrogels. Consequently, the resulting hydrogel composites had a more textured and rougher surface, unlike the calcium alginate hydrogel beads which appeared to be smoother [24]. This rough surface of composites was believed to be beneficial for adsorption as, the rougher the surface, higher the surface area and stronger the contaminant interactions.

On the other hand, the micrographs of adsorbed samples revealed the progressive structural changes owing to the presence of new irregular bulky particles over the surface. This resulted in increased protuberance which are absent before loading TOA and metal ions. After successful desorption, the microscopic observation did not show the

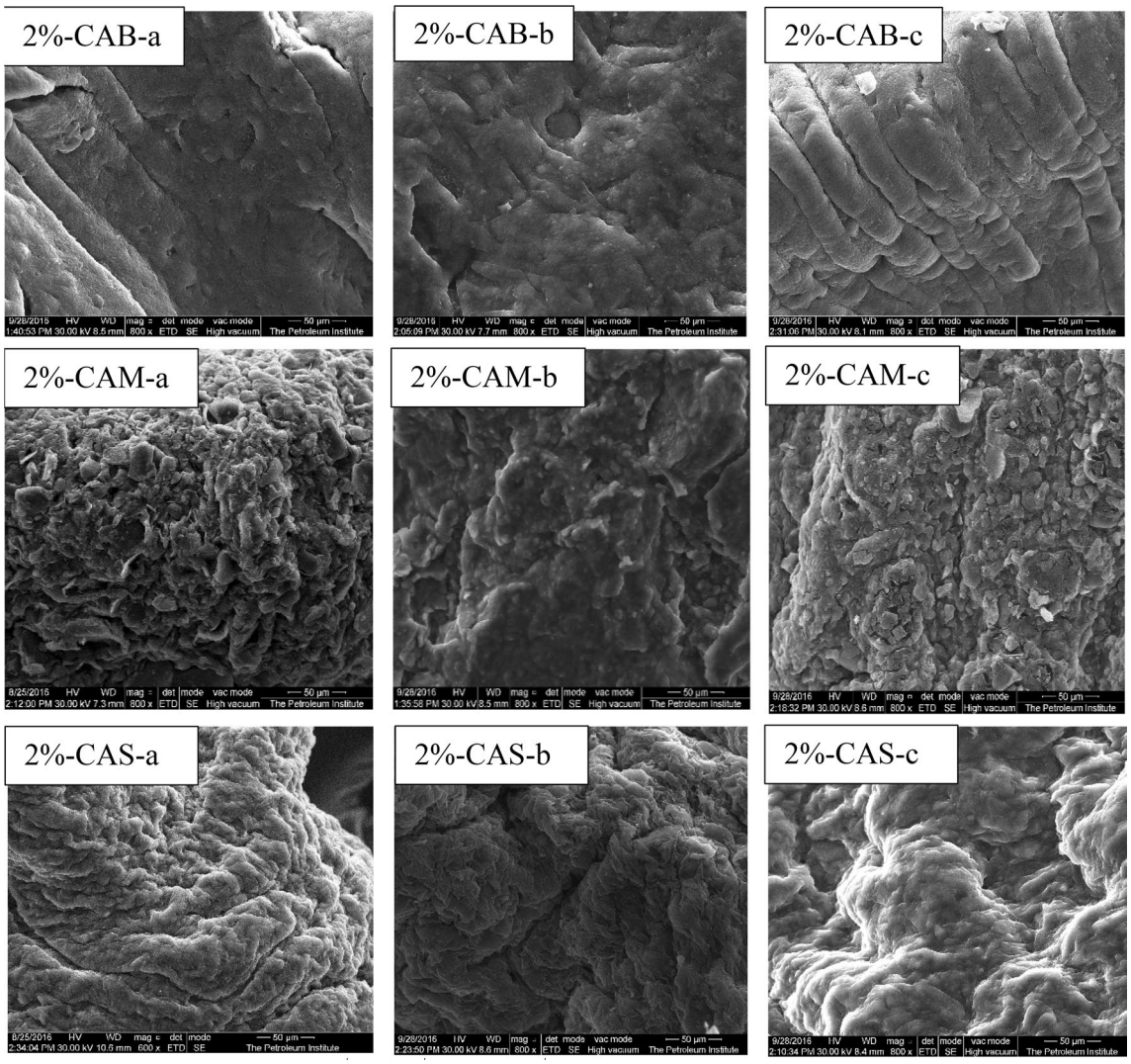

Fig. 3 SEM micrographs of Na^+-B, Na^+-M and Na^+-S clay and various CAH composites: a refers to fresh, b and c refers to adsorbed and desorbed samples after third adsorption–desorption cycle

presence of any uneven particles and the external structure was found to be similar to that of fresh composites. These, conclusions were found to be in agreement with the observations obtained from EDX analysis. Nevertheless, no change was observed in the shape of the prepared composites after adsorption and desorption, owing to the excellent mechanical strength provided by the clay material.

EDX analysis of CAH composites

Energy Dispersive X-ray analysis was carried out to assess the surface characteristic of the pristine and contaminant loaded CAH composites (Fig. 4). The distinctive signals, which are characteristics of Cr and Fe, are observed at the energy values of 5.4 and 6.4 keV and can be discovered only in Fig. 4b, the EDX spectra of adsorbed samples. Comparing the spectrum of adsorbed composites with desorbed, the absence of tiny peaks of Cr and Fe has revealed the effectiveness of the desorption process utilized. Though only a qualitative analysis can be carried out, the EDX analysis has undoubtedly demonstrated the successful adsorption and desorption of contaminants onto and from CAH composites, respectively.

FTIR analysis of CAH composites

The difference between the fresh, adsorbed and desorbed CAH composites beads were studied using FTIR analysis (Fig. 5). A consistent shift in % of transmittance was observed between the fresh CAH composites sorbents and those adsorbed with MDEA. This is ascribed to the adsorption of organic acid anions and metal ions onto the adsorbent

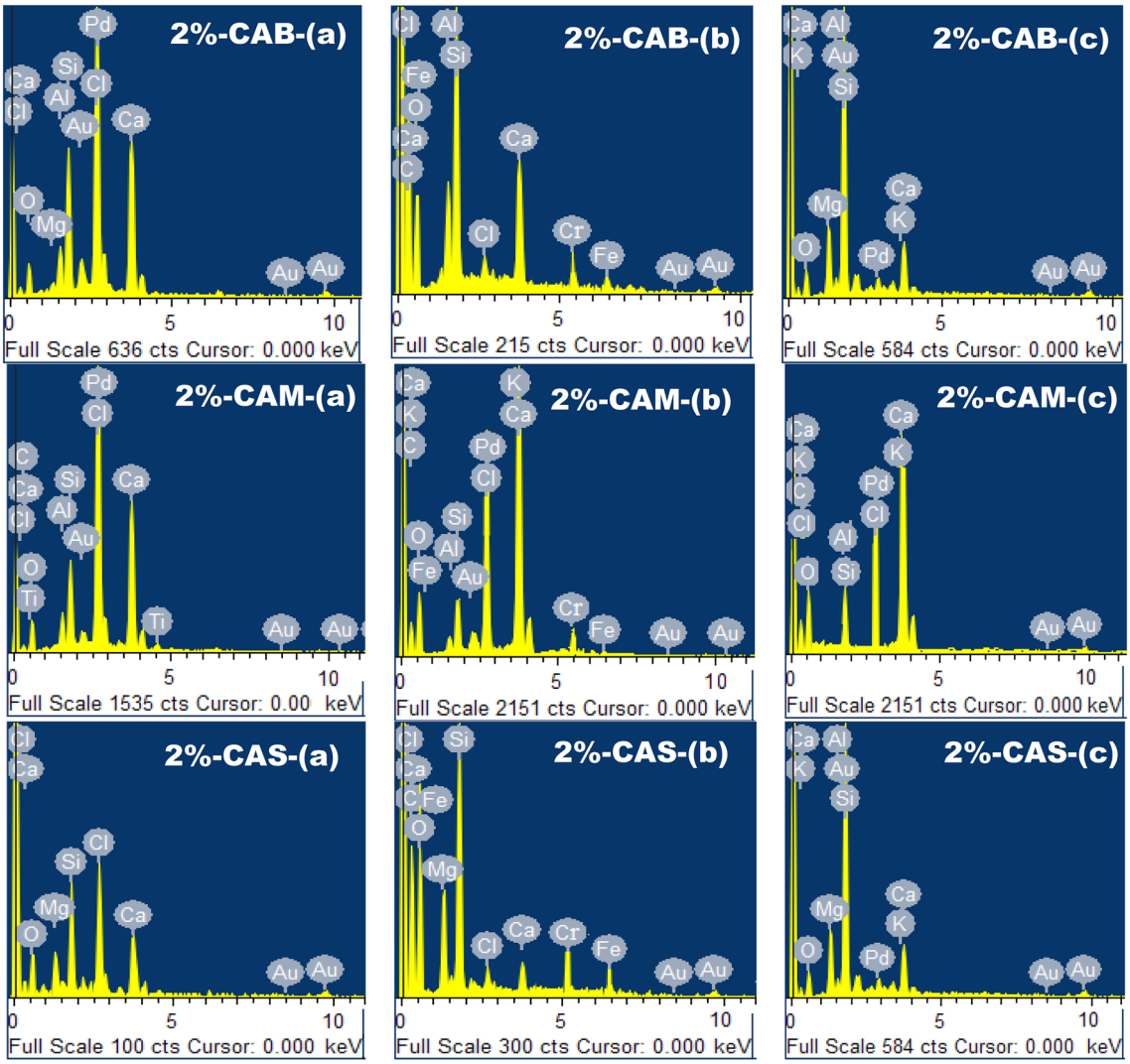

Fig. 4 EDX spectra of CAH composites: **a** refers to fresh, **b** and **c** refers to adsorbed and desorbed samples after third adsorption–desorption cycle

surface. The broad peak at 3310 cm^{-1} observed in the spectrum of fresh CAH composites attributes to the stretching and deformation vibration of the hydroxyl (–OH) groups of the weakly bound water molecule present in the alginate. Whereas the bands at 1637 cm^{-1} and 1414 cm^{-1} ascribed to the asymmetric and symmetric stretching vibrations of the carboxyl (–COOH) group present in the alginate molecule [25] and the band at 1018 cm^{-1}, indicated the C–O stretching vibration of the polysaccharides [26].

After adsorption, the bands at 3310 cm^{-1} became relatively weak owing to the complexation of the hydroxyl group with the TOA and heavy metal ions. Also, the bands at 1637 cm^{-1} and 1018 cm^{-1} became even sharper and an additional moderately intense peak was observed in the spectrum at 2955 cm^{-1} due to increase in stretching of the C–O groups from the adsorption of TOA ions. On the other hand, the peak at 1414 cm^{-1} was observed to shift to 1454 cm^{-1} and 1316 cm^{-1}. This shift in wavenumbers for adsorbed composites further indicates the coordination interaction that is taking place between the Ca^{2+} and the heavy metal ions, which induces the peak of –COO to move [27, 28].

However, in case of desorbed composites, all the peaks were observed to be similar to that of the fresh composites, providing clear evidence of the effective desorption process utilized.

Batch adsorption studies

Effect of adsorbent dosage

Figure 6 represents the effect of CAH dose on the adsorption capacity for TOA and heavy metals from industrial

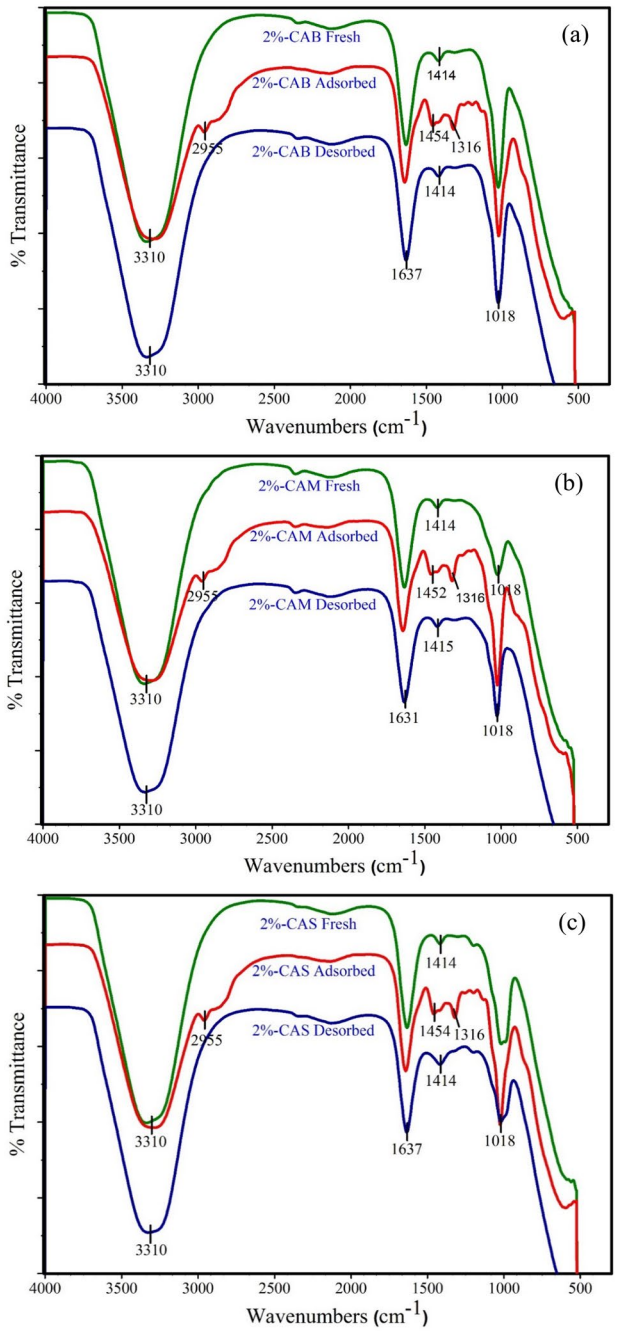

Fig. 5 FTIR of the fresh, adsorbed and desorbed CAH composites: **a** 2%-CAB, **b** 2%-CAM and **c** 2%-CAS

lean MDEA solution at 25 °C. Understanding the effect of dosage is essential as it provides an insight on the capacity of the adsorbent for a given initial contaminant concentration. The equilibrium sorption capacity of the CAH composites for all the contaminants was observed to decrease whereas the removal efficiencies increased with increasing the adsorbent dose. It can be attributed to the fact that, at lower adsorbent dose, all the active sites present on the adsorbent surface are exposed entirely resulting in faster saturation and higher equilibrium sorption capacity per unit weight of sorbent, q_e [28]. The sorption capacity for TOA (Fig. 6a) was found to decrease from 58.6 to 18.3 mg/g for 2%-CAB, 47.1–16.6 mg/g for 2%-CAM and 44.4–14.9 mg/g for 2%-CAS, when the dose of composite particles was increased from 0.5 g to 5.0 g. A similar decrease in sorption capacity was observed with increasing the sorbent dose for heavy metal removal using CAH composites (Fig. 6b, c). On the other hand, with increasing sorbent dose, the availability of higher surface area or more active sites/functional groups for sorption comparing to the limited adsorbing species available in a fixed initial adsorbate concentration resulted in increasing the removal efficiency [29]. For an adsorbent dose of 5.0 g, 2%-CAS exhibited the highest removal efficiency of TOA (44.5%) and iron (90.7%), followed by 2%-CAM (43.1% and Iron 85.4%) and 2%-CAB (36.8% and Iron 75.0%). Whereas, the highest chromium removal was achieved by 2%-CAM (74.0%), followed by 2%-CAS (70.7%) and 2%-CAB (66.5%). On the other hand, 2%-CAB exhibited the highest sorption capacity, followed by 2%-CAM and 2%-CAS. This is because as sepiolite clay are light weight, the dried weight of 2%-CAS was higher than that of 2%-CAB and 2%-CAM and as a result the uptake capacity which is calculated based on the dried weight of the adsorbent decreases.

Even though, the montmorillonite containing CAH composites had better removal efficiency than bentonite one, from economic point of view, MMT is more expensive. This is attributed to the complex and expensive process required for the extraction of MMT through the purification of the bentonite ore [30]. Hence further adsorption studies were focused on exploring the capability of 2%-CAS and 2%-CAB composites as potential contenders for industrial lean amine reclamation.

Effect of contact time

The effects of contact time on the adsorption behavior of TOA and heavy metals on 2%-CAB and 2%-CAS composites are presented in Fig. 7a. The initial rate of adsorption of both TOA and chromium was found to be rapid and the highest adsorption capacity was achieved within first 30 min. Further, the capacity was reduced slightly and gradually attained equilibrium after 4 h with a capacity almost same as that of 30 min. Conversely, in case of iron, about 72.1% and 80.18% of the sorption capacity took place within the first 30 min for 2%-CAB and 2%-CAS respectively and then progressively increased reaching equilibrium at 4 h. The pH of the solution plays an important role during the adsorption process and affect the surface charge of adsorbent, the degree of ionization, and speciation of adsorbate. The alkaline pH of the lean MDEA solution (pH 10.5) affects the

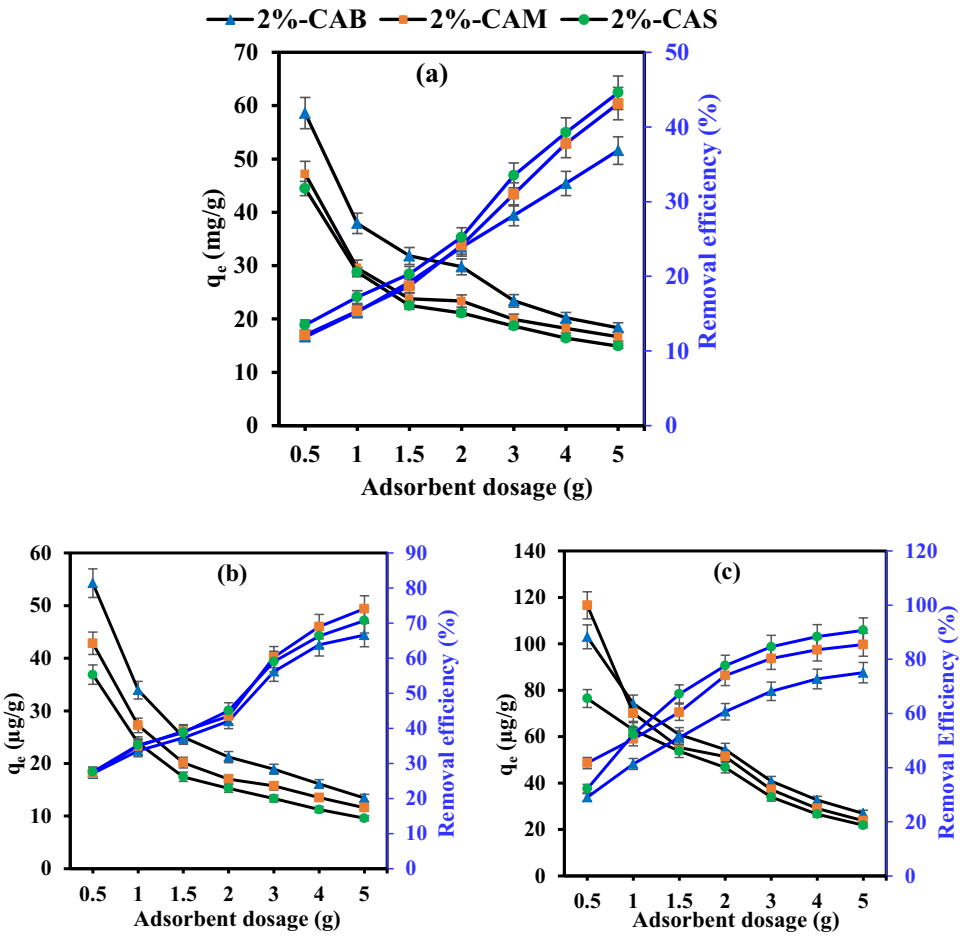

Fig. 6 Effect of adsorbent dosage on uptake capacity and % removal of **a** TOA, **b** chromium and **c** iron using various CAH composites at 25 °C

solubility of the metal ions, concentration of the counter ions on the functional groups on the alginate adsorbent and the degree of the ionization of the adsorbent during the reaction. At this pH, both the chromium (CrO_4^{2-}) and TOA remain as anionic form while iron exist as cationic form [12, 31]. Thus, iron adsorption curve was different from the adsorption of both the TOA and chromium. Both this behavior indicated that the bio-sorption of contaminants consist of three stages: (1) The initial rapid stage which is ascribed to the availability of large number of vacant adsorptive sites on the surface for binding and (2) the second stage, where with the lapse of time the adsorbate species gradually fills the available free surface through slow intra particle diffusion [32], whose contribution was relatively small and (3) finally attained equilibrium due to the decrease of adsorbate concentrations and available active sites. As a result, subsequent adsorption experiments were carried out at the optimum contact time of 4 h.

Effect of temperature

The effect of temperature on the sorption of TOA and heavy metal from industrial lean MDEA was investigated by varying the temperature from 25 to 45 °C and the results are as depicted in Fig. 7b. The adsorption data showed that the equilibrium adsorption capacity and the removal efficiency of TOA and heavy metal ions using 2%-CAB and 2%-CAS was found to increase with increasing the temperature; indicating the endothermic nature of the sorption process. This increase with higher temperature are attributed to the following aspects: (1) as the temperature rises, the attractive forces between the adsorbent surface and the contaminants strengthens and increases the sorption capacity, which supports the chemisorption nature of sorption [33]; (2) the swelling degree of the composites increases with increase in temperature and augments easy accessibility to the pores, which results in an increase in sorption capacity; and (3) at elevated temperature, the rupture of the bonds of the functional groups on the adsorbent surface may increase the number of active sites, which enhances the sorption efficiency [34].

Modeling of adsorption kinetics

Adsorption kinetics provide valuable insight for understanding the controlling mechanism of adsorption process and for

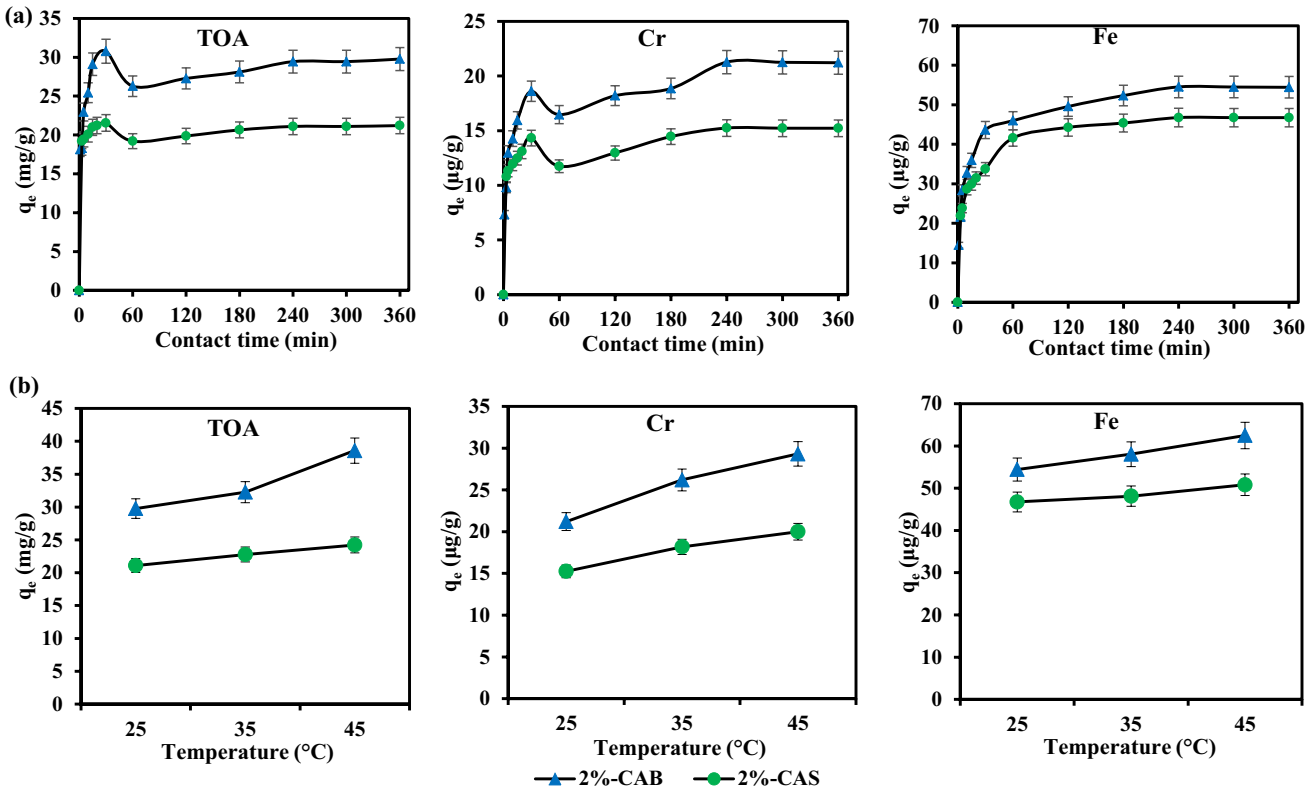

Fig. 7 Effect of **a** contact time and **b** temperature on the uptake capacity of TOA, chromium (Cr) and iron (Fe) using 2.0 g of 2%-CAB and 2%-CAS composites

predicting the adsorption rate and required equilibrium time, which are a key information for designing and modeling the process. Two different kinetics models were studied to analyze the experimental data; these included Lagergren's pseudo-first order model [35], Ho's pseudo-second order model [36]. In addition, the Weber and Morris intra-particle diffusion model [37] was further tested to determine the diffusion mechanism of the adsorption system.

1. Lagergren pseudo-first order kinetics model:

$$\ln\left(q_e - q_t\right) = \ln q_e - k_1 t \tag{4}$$

Ho's pseudo-second order kinetics model:

$$\frac{t}{q_t} = \frac{1}{k_2 q_e^2} + \frac{t}{q_e} \tag{5}$$

where q_e and q_t are the amount of TOA or heavy metal ions adsorbed on the adsorbent at equilibrium and at any time 't', respectively. k_1 is the pseudo-first order rate constant (min^{-1} for both TOA and heavy metals), k_2 is the second order rate constant (g/mg min for TOA and g/µg min for heavy metals). The larger the value of k_2, the slower is the rate of adsorption.

2. Weber and Morris intra-particle diffusion model:

$$q_t = k_i * t^{0.5} + C \tag{6}$$

where k_i is the intra-particular diffusion rate constant (mg/g $min^{0.5}$ for TOA and µg/g $min^{0.5}$ for heavy metals) and C_i is the boundary layer effect at stage. i.e. the larger the C, the greater is the boundary layer effect.

The linear plot of $\ln(q_e - q_t)$ versus t (Fig. S1) and $\frac{t}{q_t}$ versus t (Fig. S2) were drawn for determining the values of rate constants k_1 and k_2 of the pseudo-first order and pseudo-second order models, respectively. The relevant parameters such as correlation coefficients, R^2 and experimental value of $q_{e,exp}$ against $q_{e,cal}$ for both the models are demonstrated in Table 1. The pseudo-second order model showed a good fit of the experimental data by achieving a correlation coefficient closer to unity. The same trend was exhibited for both 2%-CAB and 2%-CAS composites for the adsorption of TOA anions, chromium and iron ions. Thus, the results indicates that adsorption of TOA and heavy metals ions on to the composites followed pseudo-second order kinetics model confirming chemisorption [38].

Prediction of the rate-limiting step is a crucial factor to be considered in any adsorption process. According to Weber–Morris model, the effect of intra particle diffusion was evaluated by plotting q_t versus $t^{0.5}$, from which the intra-particle diffusion constant k_i and the value of boundary

Table 1 Pseudo first and second order model parameters for the adsorption of TOA, chromium and iron onto 2.0 g of 2%-CAB and 2%-CAS composites at 25 °C

Name of composite	Name of contaminant	C_i	$q_{e,exp}$	Pseudo-first order kinetics parameters			Pseudo-second order kinetics parameters		
				k_1 (min^{-1})	$q_{e,cal}$	R^2	k_2	$q_{e,cal}$	R^2
2%-CAB	TOA	3745[a]	29.4[c]	0.01	7.6[c]	0.8178	0.01[e]	29.3[c]	0.9988
	Chromium	1517[b]	21.2[d]	0.007	7.8[d]	0.5792	0.006[f]	21.1[d]	0.9940
	Iron	2697[b]	54.5[d]	0.013	26.7[d]	0.8734	0.002[f]	55.2[d]	0.9970
2%-CAS	TOA	3745[a]	21.1[c]	0.005	1.7[c]	0.5702	0.03[e]	21.0[c]	0.9993
	Chromium	1517[b]	15.2[d]	0.006	3.1[d]	0.3968	0.011[f]	15.2[d]	0.9953
	Iron	2697[b]	46.7[d]	0.016	21.4[d]	0.9612	0.002[f]	47.8[d]	0.9994

[a]Units in mg/L, [b]units in µg/L, [c]units in mg/g, [d]units in µg/g, [e]units in g/mg min, [f]units in g/µg min

layer effect were retrieved (Fig. S3). The linear portion of the curve is used for determining the rate-limiting step of adsorption. If the plot passes through the origin; that is intercept, C is zero, then the rate determining step pertains only to intra-particle diffusion. Or else, if the plots are multi linear and can be segregated into different linear sections, then several rate-limiting steps govern the sorption mechanism [39]. In theory, the plots of the intra-particle diffusion can comprise of up to 3 linear regions, which represents the following aspects: instantaneous diffusion through boundary-layer, followed by intra-particle diffusion and finally adsorption equilibrium. Generally, these 3 regions are followed by a horizontal line that symbolizes the system at equilibrium [40]. For adsorption of TOA and heavy metals onto 2%-CAB and 2%-CAS composites, the diffusion plots presented in Fig. S3 was not linear throughout the time range and displayed 3 stages, indicating that there are several rate-controlling steps. However, for all the three contaminants, the lines of all the stages did not pass through the origin, illustrating that intra-particle diffusion was not the rate-determining step.

The values of intra-particle diffusion rate constant, k_i and C_i, which reflects the thickness of the boundary layer retrieved from intra-particle diffusion model are shown in Table 2. It was observed that values of $k_{i,1}$ for 2%-CAB and 2%-CAS were in general greater than $k_{i,2}$, $k_{i,3}$ etc. irrespective of the contaminant adsorbed. This behavior was ascribed to the resistance in the mass transfer originating from the diffusion of the contaminants into the pores as the concentration of the contaminants gradually decreases. Thus, it clearly confirms the effect of faster external surface adsorption than the intra-particle diffusion. Although intra-particle diffusion was involved in the adsorption process, the overall poor regression coefficient and the huge variation of calculated q_e from experimental q_e (Table 2) further proved that pore diffusion was not the sole mechanism applicable for the sorption of TOA and heavy metals onto CAB and CAS composites.

Adsorption isotherm

Adsorption isotherms are generally utilized to understand the interaction between the adsorbate and the adsorbent and are given by the plot of solute concentration, q_e (mg/g or µg/g) in the sorbent as function of the solute concentration in the solution, C_e (mg/L or µg/L) at equilibrium (Fig. 8). For both 2%-CAB and 2%-CAS, the adsorption of TOA and heavy metals followed a type VI isotherm, indicating multi-layer adsorption process. 2%-CAS composites exhibited higher removal for TOA and heavy metals such as chromium and iron from industrial lean MDEA solution when compared to that of 2%-CAB owing to the presence of hollow brick-like fibrous structured sepiolite that has great potential for retaining of micro-pollutants [41]. Even though 2%-CAS exhibited almost similar TOA and Chromium removal efficiency when compared to 2%-CAB, the uptake capacity of 2% CAB which was calculated based on the dried mass of the adsorbent outweighed 2%-CAS. This is because for a given weight, 2%-CAS contains more number of beads than 2%-CAB and as a result the dried weight of 2%-CAS was higher than that of 2%-CAB.

Desorption studies

Reusability of the adsorbent is of great importance as the overall cost associated with the adsorption process depends on the regeneration capability of the adsorbent. The results (Fig. 9a) of desorption experiments performed using various concentration of $CaCl_2$ as eluent confirms that 4% $CaCl_2$ or used $CaCl_2$ (left over solution after polymerization) was effective for regaining the sorption capacity of CAH composites for TOA, chromium and iron from industrial lean MDEA solutions.

Figure 9b further depicts the excellent recyclability of 2%-CAS and 2%-CAB composite adsorbents. After three consecutive adsorption and desorption cycles, 2%-CAS composites exhibited the highest removal efficiency with

Table 2 Stage-wise and overall intra-particle diffusion model parameters for the adsorption of TOA, chromium and iron onto 2.0 g of 2%-CAB and 2%-CAS composites at 25 °C

Name of composite	Name of contaminant	C_i	$q_{e,exp}$	Intra-particle diffusion model parameters		
				k_i	$q_{e,cal}$	R^2
2%-CAB	TOA					
	Stage I	3745[a]	29.4[c]	0.005[e]	4.4[c]	1
	Stage II			0.003[e]	3.4[c]	0.9092
	Stage III			0.002[e]	2.7[c]	0.9639
	Overall			0.01[e]	2.0[c]	0.4387
	Chromium					
	Stage I	1517[b]	21.2[d]	2.9[f]	0.2[d]	1
	Stage II			0.3[f]	0.5[d]	0.9946
	Stage III			0.02[f]	1.8[d]	0.9446
	Overall			0.03[f]	1.5[d]	0.9325
	Iron					
	Stage I	2697[b]	54.5[d]	40.3[f]	0.08[d]	0.9918
	Stage II			1.2[f]	0.2[d]	0.9998
	Stage III			0.03[f]	0.9[d]	0.8729
	Overall			0.2[f]	0.4[d]	0.8232
	TOA					
2%-CAS	Stage I	3745[a]	21.1[c]	0.02[e]	1.5[c]	0.9875
	Stage II			0.01[e]	2.8[c]	0.9991
	Stage III			0.002[e]	4.6[c]	0.9572
	Overall			0.0001[e]	17.1[c]	0.1419
	Chromium					
	Stage I	1517[b]	15.2[d]	0.6[f]	1.2[d]	0.9764
	Stage II			0.1[f]	0.8[d]	0.9984
	Stage III			0.01[f]	2.5[d]	0.9526
	Overall			0.004[f]	4.2[d]	0.6931
	Iron					
	Stage I	2697[b]	46.7[d]	1.7[f]	0.2[d]	0.9953
	Stage II			0.2[f]	0.4[d]	0.9983
	Stage III			0.008[f]	1.8[d]	0.9473
	Overall			0.1[f]	0.5[d]	0.9072

[a]Units in mg/L, [b]units in μg/L, [c]units in mg/g, [d]units in μg/g, [e]units in mg/g $min^{0.5}$, [f]units in μg/g $min^{0.5}$

24.9% for TOA ions, 45.1% for chromium ions, and 77.6% for iron, respectively. No reduction in desorption efficiency was observed even after 3 consecutive cycles; proving the outstanding reusability of the CAH composite sorbents.

Furthermore, a batch mode of desorption studies were carried out at room temperature (25 °C) using the total amount of 2%-CAB composites (17.0 g) which was loaded with contaminants from the previously performed batch sorption experiment. Even after consequent 3 adsorption–desorption cycles (Fig. S4), no reduction in adsorption capacity was observed for TOA and heavy metals. Additionally, no significant changes in the structure was noticed in these composites, despite its high water content (95.0%). This could be ascribed to the high mechanical strength imparted by the addition of clay as fillers in the composites. Thus undoubtedly, CAH composites developed using Bentonite and Sepiolite clay proves to be an efficient adsorbent material for industrial lean MDEA reclamation.

Foaming studies

Foaming experiments of industrial lean amine (before and after adsorptive treatment) were carried out using the foam fractionator with the objective of investigating the effect of removal of TOA and heavy metal ions on the foaming behavior of aqueous MDEA. To compare the foaming behavior, foaming experiments were conducted in the foam fractionation column using both untreated and adsorbed lean MDEA. The treated lean MDEA were obtained by suspending 12.0 g of 2%-CAS composites in 120 mL of lean MDEA solution (maintaining weight by volume ratio of 1:10) and allowing it to equilibrate on a water bath shaker at 140 rpm for 4 h.

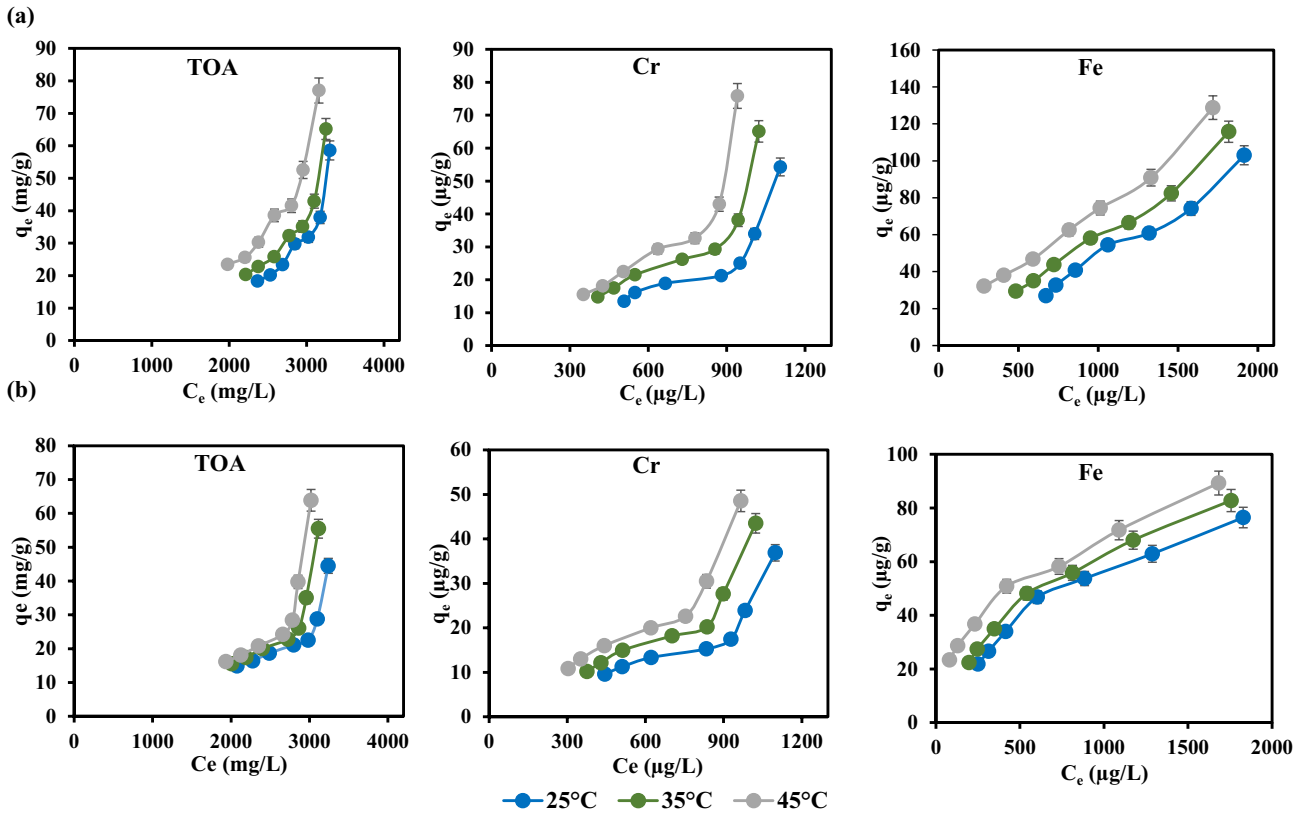

Fig. 8 Adsorption equilibrium curve, q_e versus C_e for the adsorptive removal of TOA, Chromium (Cr) and Iron (Fe) using **a** 2%-CAB and **b** 2%-CAS composites

After reaching equilibrium, the lean MDEA samples were filtered to remove the adsorbent particles left in the solution and used for foaming studies. The amount of TOA left in the treated MDEA were quantified using UV–Vis spectrophotometer and a reduction of 15.8% in TOA content was noted.

In a typical foaming experiment, 120 mL of feed solution were filled into the foam raiser. Once the required liquid level was attained in the bottom of the foam raiser, dry air was sparged through the gas distributor into the liquid pool. The volume of the foam generated was measured in terms of its foam height. Analysis of the foaming experiments (Fig. 10) revealed that the untreated industrial lean MDEA exhibited the highest foaming tendency by attaining a foam volume of 120 mL; the entire 120 mL of feed MDEA foamed completely without leaving any residual solution in the foam fractionator column. However, for adsorptive treated MDEA, the foam height reached only a value of 75 mL; a decrease of 37.5% in foam height compared to untreated lean MDEA. Different batch of industrial lean MDEA solutions with different concentrations of TOA were used to obtain similar trend of foaming results. These findings further confirms the effectiveness of the TOA removal achieved by the alginate/clay composite adsorbents on the foaming behavior of industrial lean MDEA.

Conclusion

In this study, the effect of adsorptive removal of TOA anions and heavy metal ions using calcium alginate clay composites on the foaming behavior of industrial lean MDEA have been examined. The equilibrium batch adsorption experiments conducted using calcium alginate/clay hybrid (CAH) composites demonstrated the extraordinary adsorption capacities exhibited by these composites for TOA and heavy metals removal from industrial lean amine. The addition of bentonite and sepiolite as reinforcing fillers not only increased the mechanical strength but also played a major role in improving the sorption performance, with 2%-CAB composites exhibiting the highest uptake capacity. Experimental results demonstrated that increasing the adsorbent dosage increased the removal efficiency with 5.0 g of composite giving the highest removal for all contaminants. Kinetics assessment indicated the rapid adsorption behavior exhibited by the composites with chemisorption in nature. Increasing temperature enhanced the adsorption efficiency owing to the increase in attractive forces between the adsorbent and the contaminants with isotherms following type IV behavior. The reusability experiments showed that the composites has excellent

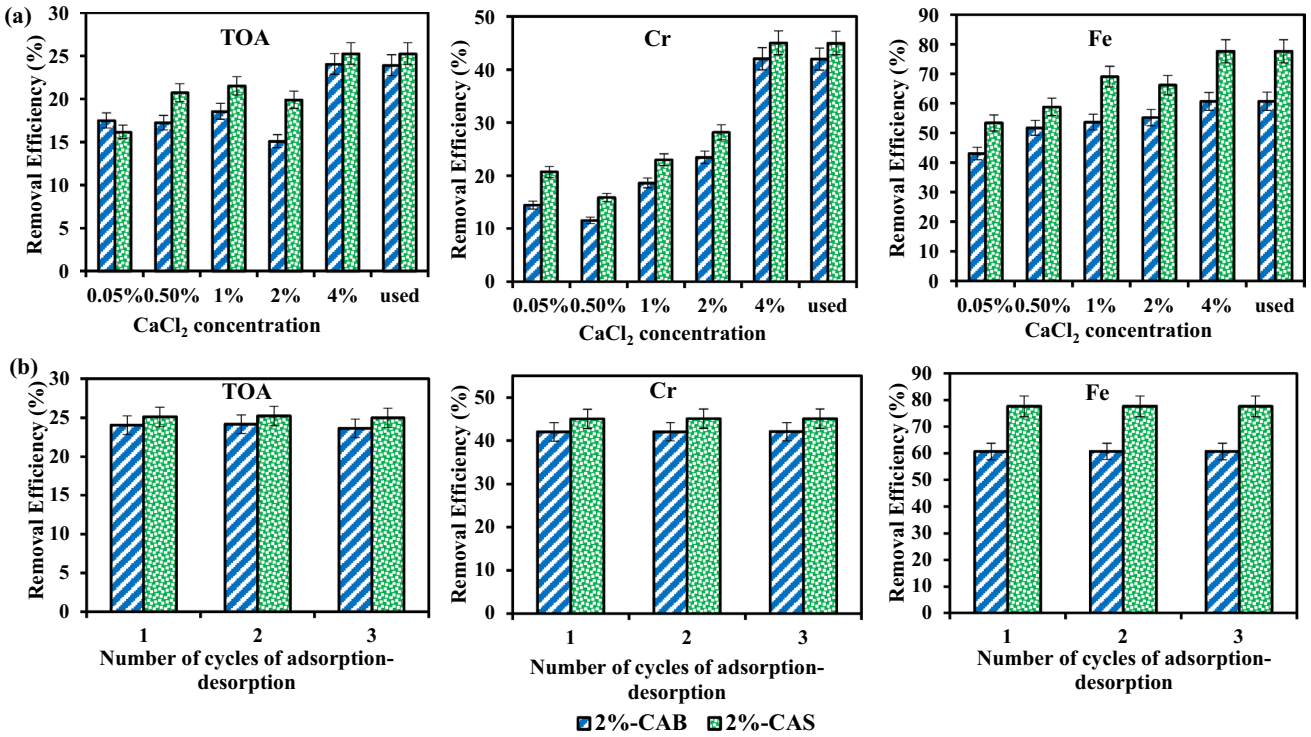

Fig. 9 Effect of **a** different $CaCl_2$ concentration as desorbing agent and **b** number cycles of regeneration on the adsorptive removal of TOA, chromium (Cr) and iron (Fe) using 2.0 g of 2%-CAB and 2%-CAS composites

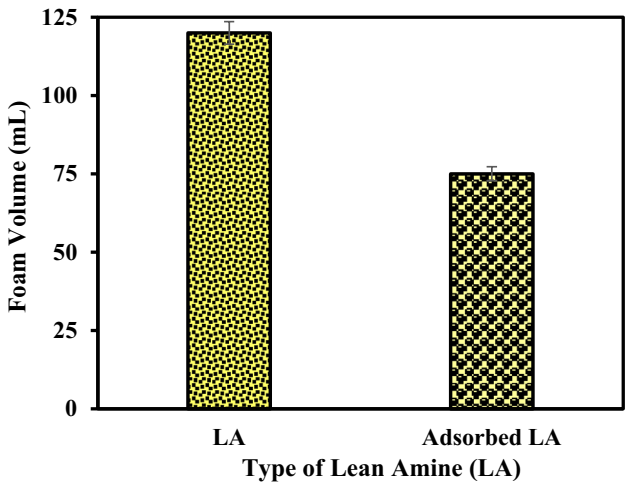

Fig. 10 Foam volume with types of lean amine

adsorption–desorption efficiency and can be used without any reduction in removal efficiency up to 3 cycles. Foaming studies conducted for adsorbed lean MDEA revealed that a 15.8% decrease in TOA content resulted in a 37.5% reduction in foam height owing to the effective removal of TOA foam creator from lean MDEA. Therefore, the reduction in the foaming tendency for adsorbed MDEA confirmed the potential advantage offered by the alginate clay composites in solving the foaming problem associated with alkanolamine based absorption processes.

Acknowledgements The authors would like to acknowledge the support provided by the Gas Research Center (GRC) at Khalifa University under research Grant GRC11006.

References

1. Cummings AL, Smith GD, Nelsen DK (2007) Advances in amine reclaiming—why there's no excuse to operate a dirty amine system. In Laurance Reid gas conditioning conference, Citeseer
2. Haws R (2001) Contaminants in amine gas treating. CCR Technologies Inc, Houston, p 11375
3. Rooney P, Bacon T, DuPart M (1996) Effect of heat stable salts on MDEA solution corrosivity. Hydrocarb Process 75(3):95–103
4. Hajilary N, Nejad AE, Sheikhaei S, Foroughipour H (2011) Amine gas sweetening system problems arising from amine replacement and solutions to improve system performance. J Pet Sci Tech 1(1):24–30

5. Liu H, Dean J, Bosen SF (1995) Neutralization technology to reduce corrosion from heat stable amine salts. In: Corrosion-national association of corrosion engineers annual conference, NACE
6. Millard M, Beasley T (1993) Contamination consequences and purification of gas treating chemicals using vacuum distillation. In: Millard MG, Beasley T (eds) Proceedings of 43 rd annual Laurance Reid gas conditioning conference, Norman, OK, March 1–3, pp 183–198
7. Burns D, Gregory RA (1995) The UCARSEP™ process for on-line removal of non-regenerable salts from amine units. IN: Proceedings of Laurance Reid gas conditioning conference. Norman, OK, USA (26 February–1 March). Citeseer
8. Meng H, Zhang S, Li C, Li L (2008) Removal of heat stable salts from aqueous solutions of *N*-methyldiethanolamine using a specially designed three-compartment configuration electrodialyzer. J Membr Sci 322(2):436–440
9. Parisi P, Bosen S (2006) Amine reclamation with minimal operational impact through electrodialysis. In: Proceedings of the Laurance Reid gas conditioning conference, p 301
10. Coberly SH, Laven TH, Cummings AL (1998) Amine heat stable salt removal from Type II anion exchange resin. Google Patents
11. Keller A, Kammiller R, Veatch F, Cummings A, Thompsen J, Mecum S (1992) Heat-stable salt removal from amines by the HSSX process using ion exchange. In: Proceedings of 42nd annual Laurance Reid gas conditioning conference. The University of Oklahoma OK, pp 61–92
12. Pal P, Banat F (2014) Comparison of heavy metal ions removal from industrial lean amine solvent using ion exchange resins and sand coated with chitosan. J Nat Gas Sci Eng 18:227–236
13. Pal P, Banat F (2015) Removal of contaminants from industrial lean amine solvent using polyacrylamide hydrogels optimized by response surface methodology. Adsorpt Sci Technol 33(1):9–24
14. Pal P, Banat F, AlShoaibi A (2013) Adsorptive removal of heat stable salt anions from industrial lean amine solvent using anion exchange resins from gas sweetening unit. J Nat Gas Sci Eng 15:14–21
15. Pal P, Banat F (2014) Contaminants in industrial lean amine solvent and their removal using biopolymers: a new aspect. J Phys Chem Biophys 4(1):1
16. Pal P, Edathil AA, Banat F (2014) Removal of total organic acid anions and heavy metal ions from industrial lean amine solvent using biopolymeric calcium alginate. In AIChE annual meeting, Atlanta, USA, AIChE, p 751f
17. Gacesa P (1988) Alginates. Carbohydr Polym 8(3):161–182
18. Aichour A, Zaghouane-Boudiaf H, Iborra CV, Polo MS (2018) Bioadsorbent beads prepared from activated biomass/alginate for enhanced removal of cationic dye from water medium: kinetics, equilibrium and thermodynamic studies. J Mol Liq 256:533–540
19. Pettignano A, Tanchoux N, Cacciaguerra T, Vincent T, Bernardi L, Guibal E, Quignard F (2017) Sodium and acidic alginate foams with hierarchical porosity: preparation, characterization and efficiency as a dye adsorbent. Carbohydr Polym 178:78–85
20. Sellaoui L, Soetaredjo FE, Ismadji S, Benguerba Y et al (2018) Equilibrium study of single and binary adsorption of lead and mercury on bentonite-alginate composite: experiments and application of two theoretical approaches. J Mol Liq 253:160–168
21. Pal P, Edathil AA, Banat F (2018) Calcium alginate gel and hard beads for the removal of total organic acid anions and heavy metal ions from industrial lean methyldiethanolamine solvent. Polym Bull. https://doi.org/10.1007/s00289-018-2376-0
22. Edathil AA, Pal P, Banat F (2018) Alginate clay hybrid composite adsorbents for the reclamation of industrial lean methyldiethanolamine solutions. Appl Clay Sci 156:213–223
23. Alhseinat E, Pal P, Keewan M, Banat F (2014) Foaming study combined with physical characterization of aqueous MDEA gas sweetening solutions. J Nat Gas Sci Eng 17:49–57
24. Tzu TW, Tsuritani T, Sato K (2013) Sorption of Pb(II), Cd (II), and Ni (II) toxic metal ions by alginate-bentonite. J Environ Protect 4(1B):51
25. Papageorgiou SK, Kouvelos EP, Favvas EP, Sapalidis AA, Romanos GE, Katsaros FK (2010) Metal–carboxylate interactions in metal–alginate complexes studied with FTIR spectroscopy. Carbohydr Res 345(4):469–473
26. Sujana M, Mishra A, Acharya B (2013) Hydrous ferric oxide doped alginate beads for fluoride removal: adsorption kinetics and equilibrium studies. Appl Surf Sci 270:767–776
27. Tripathy T, Singh R (2001) Characterization of polyacrylamide-grafted sodium alginate: a novel polymeric flocculant. J Appl Polym Sci 81(13):3296–3308
28. Zhou Q, Lin X, Li B, Luo X (2014) Fluoride adsorption from aqueous solution by aluminum alginate particles prepared via electrostatic spinning device. Chem Eng J 256:306–315
29. Tumin ND, Chuah AL, Zawani Z, Rashid SA (2008) Adsorption of copper from aqueous solution by Elais Guineensis kernel activated carbon. J Eng Sci Tech 3(2):180–189
30. Utracki LA (2004) Clay-containing polymeric nanocomposites: iSmithers. Rapra Publishing, Shropshire
31. Onchoke KK, Janusa MA, Sasu SA (2015) Evaluation of the performance of a rural municipal wastewater treatment plant in Nacogdoches, East Texas (USA). Chem Ecol 31:567–582
32. Jiang F, Dinh DM, Hsieh YL (2017) Adsorption and desorption of cationic malachite green dye on cellulose nanofibril aerogels. Carbohydr Polym 173:286–294
33. Horsfall Jnr M, Spiff AI (2005) Effects of temperature on the sorption of $Pb2^{+}$ and Cd^{2+} from aqueous solution by *Caladium bicolor* (Wild Cocoyam) biomass. Electron J Biotechnol 8(2):43–50
34. Figaro S, Avril J, Brouers F, Ouensanga A, Gaspard S (2009) Adsorption studies of molasse's wastewaters on activated carbon: modelling with a new fractal kinetic equation and evaluation of kinetic models. J Hazard Mater 161(2):649–656
35. Lagergren S (1898) About the theory of so-called adsorption of soluble substances. Kung Sven Veten Hand 24:1–39
36. Ho YS, McKay G (1999) Pseudo-second order model for sorption processes. Process Biochem 34:451–465
37. Weber WJ, Morris JC (1963) Kinetics of adsorption on carbon from solution. J Sanit Eng Div 89:31–60
38. Sun X, Chen JH, Su Z, Huang Y, Dong X (2016) Highly effective removal of Cu (II) by a novel 3-aminopropyltriethoxysilane functionalized polyethyleneimine/sodium alginate porous membrane adsorbent. Chem Eng J 290:1–11
39. Doğan M, Özdemir Y, Alkan M (2007) Adsorption kinetics and mechanism of cationic methyl violet and methylene blue dyes onto sepiolite. Dyes Pig 75(3):701–713
40. Kilic M, Apaydin-Varol E, Pütün AE (2011) Adsorptive removal of phenol from aqueous solutions on activated carbon prepared from tobacco residues: equilibrium, kinetics and thermodynamics. J Hazard Mater 189(1):397–403
41. Adeyemo AA, Adeoye IO, Bello OS (2015) Adsorption of dyes using different types of clay: a review. Appl Water Sci 7:543–568